ISSN 0965-5425, Computational Mathematics and Mathematical Physics, 2006, Vol. 46, No. 8, pp. 1418–1441. © MAIK "Nauka/Interperiodica" (Russia), 2006.
Original Russian Text © O.M. Belotserkovskii, Yu.I. Khlopkov, 2006, published in Zhurnal Vychislitel'noi Matematiki i Matematicheskoi Fiziki, 2006, Vol. 46, No. 8, pp. 1494–1518.

Monte Carlo Methods in Applied Mathematics and Computational Aerodynamics

O. M. Belotserkovskii[a] and Yu. I. Khlopkov[b]

[a] *Institute of Automated Design, Russian Academy of Sciences, Vtoraya Brestskaya ul. 18/2, Moscow, 123056 Russia*

[b] *Zhukovsky Central Institute of Aerohydrodynamics, ul. Zhukovskogo 1, Zhukovskii, Moscow oblast, 140186 Russia*

e-mail: khlopkov@falt.ru

Received February 7, 2006

Dedicated to the memory of a prominent expert in Monte Carlo methods and their applications in fluid dynamics, V. E. Yanitskii (1941–2001).

Abstract—A survey of the Monte Carlo methods developed in the computational aerodynamics of rarefied gases is given, and application of these methods in unconventional fields is described. A short history of these methods is presented, and their advantages and drawbacks are discussed. A relationship of the direct statistical simulation of aerodynamical processes with the solution of kinetic equations is established; it is shown that the modern stage of the development of computational methods is impossible without the use of the complex approach to the development of algorithms with regard for all the specific features of the problem to be solved (its physical nature, mathematical model, the theory of computational mathematics, and stochastic processes). Possible directions of the development of the statistical simulation methods are discussed.

DOI: 10.1134/S0965542506080124

Keywords: Monte Carlo method, computational aerodynamics, survey of computational methods

1. INTRODUCTION

The appearance of statistical simulation (Monte Carlo) methods in various fields of applied mathematics is usually caused by the appearance of qualitatively new practical problems. The examples include the creation of nuclear weapons, space development, the study of atmospheric optics phenomena, and the study of physicochemical and turbulence processes. One good definition is as follows: The Monte Carlo methods are the methods designed for solving mathematical problems (e.g., systems of algebraic, differential, or integral equations) based on the direct statistical simulation of physical, chemical, biological, economic, social, and other processes using the generation and transformation of random variables.

The first paper devoted to the Monte Carlo method was published as early as in 1873 [1]. It described the experimental determination of π by a realization of the stochastic process of tossing a needle on a sheet of ruled paper. A striking example is the use of von Neumann's idea to simulate the neutron trajectories in the Los Alamos laboratory in the 1940s. Although the Monte Carlo methods require a large amount of computations, the absence of computers at that time did not discourage the researchers. The name of these methods comes from the capital of the Principality of Monaco, which is famous for its Casino; indeed, the roulettes used in the casino are perfect tools for generating random numbers. The first paper [2] that systematically expanded this method was published in 1949. In that paper, the Monte Carlo method was used to solve linear integral equations. It could easily be guessed that these equations were related to the problem of the passage of neutrons through matter. In Russia, studies concerning the Monte Carlo methods appeared after the Geneva International Conference on the Peaceful Uses of Atomic Energy. One of the first Russian studies is [3].

The general scheme of the Monte Carlo method is based on the central limit theorem, which states that the random variable $Y = \sum_{i=1}^{N} X_i$ equal to the sum of a large number of random variables with the same expectation m and the same variance σ^2 has the normal distribution with the expectation N and the variance $N\sigma^2$. Assume that we want to solve an equation or find the result of a certain process I. If we can construct

the random variable ξ with the probability density $p(\mathbf{x})$ such that the expectation of this variable is equal to the unknown solution $\mathbf{M}(\xi) = I$, then we obtain a simple method for estimating the solution and its error:

$$I = \mathbf{M}(\xi) \approx \frac{1}{N}\sum_{i=1}^{N}\xi_i \pm \frac{3\sigma}{\sqrt{N}}.$$

This implies the following general properties of the Monte Carlo methods:

(1) The absolute convergence to the solution with the rate $1/N$.

(2) An unfavorable dependence of the error ε on the number of trials: $\varepsilon \approx 1/\sqrt{N}$ (to reduce the error by an order of magnitude, the number of trials must by increased by two orders of magnitude).

(3) The main method of reducing the error is the variance reduction; in other words, this is a good choice of the probability density $p(\mathbf{x})$ of the random variable ξ in accordance with the physical and mathematical formulation of the problem.

(4) The error is independent of the dimensionality of the problem.

(5) A simple structure of the computation algorithm (the computations needed to realize a proper random variable are repeated N times).

(6) The structure of the random variable ξ can be generally based on a physical model of the process that does not require a formulation of the controlling equations as in regular methods; this fact is increasingly important for modern problems.

We illustrate the main features of the Monte Carlo methods and the conditions under which these methods outperform the conventional finite difference methods or are inferior to them using the following example. Suppose that we want to evaluate the definite integral of a continuous function over the interval $[a, b]$:

$$I = \int_a^b f(x)dx.$$

To evaluate this integral using the Monte Carlo method, we construct a random variable ξ with the probability density $p(x)$ such that its expectation

$$\mathbf{M}(\xi) = \int_{-\infty}^{\infty}\xi p(x)dx$$

is equal to I. Now, if we set $\xi = f(\mathbf{x})/p(\mathbf{x})$ within the integration limits, then we have, by the central limit theorem,

$$I = \frac{1}{N}\sum_{i=1}^{N}\xi_i \pm \frac{3\sigma}{\sqrt{N}}. \quad (1)$$

On the one hand, the evaluation of I by formula (1) can be interpreted as the solution of a mathematically stated problem; on the other hand, it can be interpreted as a direct simulation of the area under the plot of $f(\mathbf{x})$. The evaluation of the one-dimensional integral I_1 by the Monte Carlo method corresponds to the computation of I using the rectangular rule with the step $\Delta x \approx 1/\sqrt{N}$ and an error $O(\Delta\mathbf{x})$. If $f(x)$ is sufficiently "good," the integral I_1 in the one-dimensional case can be calculated accurate to $O(\Delta x^2)$ using the trapezoid rule, accurate to $O(\Delta x^3)$ using the parabolic rule, and to any desired accuracy without a considerable increase in the computational effort. In the multidimensional case, the difficulties in using schemes of a high order of accuracy increase; for this reason, they are rarely used for the calculation of n-dimensional integrals I_n for $n \geq 3$.

Let us compare the efficiency of the regular and statistical methods for the problem described above. Let n be the dimensionality of the problem, Y be the number of nodes on an axis, $R = Y^n$ be the total number of nodes for the regular methods, q be the order of accuracy, N be the number of statistical trials, and ν be the number of operations needed to process one node (to perform one statistical trial). Then, $\varepsilon_L = Y^{-q}$ is the error of the regular methods, $\varepsilon_K = N^{-1/2}$ is the error of the statistical methods, $L(\varepsilon) = \nu R = \nu\varepsilon_L^{-n/q}$ is the number of operations when the problem is solved by a regular method, and $K(\varepsilon) = \nu N = \nu\varepsilon_K^{-2}$ is the number of opera-

tions when the problem is solved by the Monte Carlo method. Then, in the case of an equal number of operations needed to obtain a solution with the same accuracy using each of the methods, we have

$$n = 2q.$$

Therefore, for $n \geq 3$ and $q = 1$ (first-order schemes), the Monte Carlo methods are preferable. For other classes of problems, the relation between the efficiency of the methods can be different.

2. THE MONTE CARLO METHODS IN COMPUTATIONAL AERODYNAMICS

Under the assumption of binary collisions and the molecular chaos hypothesis, the dynamics of a rarefied gas is described by the Boltzmann integro-differential kinetic equation for the single-particle distribution density:

$$\frac{\partial f}{\partial t} + \boldsymbol{\xi}\nabla f = \int (f' f_1' - f f_1)\mathbf{g} b db d\varepsilon d\boldsymbol{\xi}_1. \tag{2}$$

Here, $f(t, x, y, z, \xi_x, \xi_y, \xi_z)$ is the distribution density. f, f_1 and f', f_1' correspond to the molecules with the velocities $\boldsymbol{\xi}, \boldsymbol{\xi}_1$ and $\boldsymbol{\xi}', \boldsymbol{\xi}_1'$ before and after the collision, $\mathbf{g}$ is the relative velocity of the molecules in binary collisions ($\mathbf{g} = |\boldsymbol{\xi} - \boldsymbol{\xi}_1|$), and b and ε are the impact parameter and the azimuth angle for the collision.

The complex nonlinear structure of the collision integral and the large number of variables (seven in the general case) present severe difficulties for the analysis including the numerical analysis. The high dimension, the probabilistic nature of the kinetic processes, and complex molecular interaction models are the natural prerequisites for the application of the Monte Carlo methods. Historically, the numerical statistical methods in rarefied gas dynamics developed in three directions:

(1) The use of the Monte Carlo methods to evaluate the collision integrals in the regular finite difference schemes for solving the kinetic equations.

(2) The direct statistical simulation of physical phenomena, which is subdivided into two approaches: the simulation of trajectories of test particles by the Haviland method [4] and the simulation of the evolution of the ensemble of particles by the Bird method [5].

(3) The construction of a stochastic process using the Ulam–Neumann procedure [6] corresponding to the solution of the kinetic equation.

The hierarchy of levels of the description of large molecular systems includes a wide range of approaches, and various descriptions of the molecular dynamics at different levels can be used for constructing efficient statistical simulation methods.

The most detailed level of description is a dynamical system. To describe a system consisting of a large number N of particles (a molecular gas is a system of this kind), one must specify the initial coordinates and velocity of each molecule $\mathbf{r}_j, \boldsymbol{\xi}_j$ and the evolution equations of this system

$$m\frac{d^2\mathbf{r}_j}{dt^2} = \sum_{i \neq j}^{N} \mathbf{R}_{ij}. \tag{3}$$

The solution of such a system is an unrealizable (cannot be solved in practice) problem even for a very rarefied gas. Indeed, at a height of 400 km (the most popular satellite orbits), one cubic centimeter contains 10^9 molecules. For this reason, a less detailed statistical description is used.

Following the Gibbs formalism, rather than consider a single system, an ensemble of systems in the $6N$-dimensional Γ-space distributed according to the N-particle distribution function $F(t, \mathbf{r}_1, \ldots, \mathbf{r}_N, \boldsymbol{\xi}_1, \ldots, \boldsymbol{\xi}_N) = F_N$ is considered. This function is interpreted as the probability of finding the system in the neighborhood $d\mathbf{r}_1 \ldots d\mathbf{r}_N d\boldsymbol{\xi}_1 \ldots d\boldsymbol{\xi}_N$ of the point $\mathbf{r}_1, \ldots, \mathbf{r}_N, \boldsymbol{\xi}_1, \ldots, \boldsymbol{\xi}_N$ at the moment t:

$$dW = F_N d\mathbf{r}_1 \ldots d\mathbf{r}_N d\boldsymbol{\xi}_1 \ldots d\boldsymbol{\xi}_N.$$

Such an ensemble is described by the Liouville equation

$$\frac{\partial F_N}{\partial t} + \sum_{i=1}^{N} \boldsymbol{\xi}_i \frac{\partial F_N}{\partial \mathbf{r}_i} + \sum_{i \neq j}^{N}\sum_{i=1}^{N} \frac{\mathbf{R}_{ij}}{m}\frac{\partial F_N}{\partial \boldsymbol{\xi}_i} = 0. \tag{4}$$

From now on, the Liouville equation and all the subsequent kinetic equations following from the Bogolyubov chain including the last Boltzmann equation have a probabilistic nature. Although Eq. (4) is simpler

than system (3), it takes into account the collisions of N molecules and is very difficult to analyze. A less detailed description is achieved by roughening the description using s-particle distribution functions $F_s = \int F_N\, d\mathbf{r}_{s+1}\ldots d\mathbf{r}_N d\boldsymbol{\xi}_{s+1}\ldots d\boldsymbol{\xi}_N$, which determine the probability to simultaneously find s particles independently of the state of the remaining $N - s$ particles.

Following Bogolyubov's ideas, we obtain the chain of linked equations

$$\frac{\partial F_s}{\partial t} + \sum_{i=1}^{s} \boldsymbol{\xi}_i \frac{\partial F_s}{\partial \mathbf{r}_i} + \sum_{i=1}^{s}\sum_{j\neq i}^{s} \frac{\mathbf{R}_{ij}}{m}\frac{\partial F_s}{\partial \boldsymbol{\xi}_i} = -\sum_{i=1}^{s}(N-s)\frac{\partial}{\partial \boldsymbol{\xi}_i}\int \frac{\mathbf{R}_{is+1}}{m} F_{s+1}\, d\mathbf{r}_{s+1}\, d\boldsymbol{\xi}_{s+1}, \tag{5}$$

up to the single-particle distribution function $F_1 = f(t, \mathbf{r}, \boldsymbol{\xi})$ corresponding to the Boltzmann gas, which only takes into account the binary collisions:

$$\frac{\partial f}{\partial t} + \boldsymbol{\xi}\frac{\partial f}{\partial \mathbf{r}} + \frac{\mathbf{R}_{12}}{m}\frac{\partial f}{\partial \boldsymbol{\xi}} = -\frac{\partial}{\partial \boldsymbol{\xi}}\int \frac{\mathbf{R}_{12}}{m} F_2\, d\mathbf{r}_1 d\boldsymbol{\xi}_1.$$

Following Boltzmann, we assume that the molecules are spherically symmetric and accept the molecular chaos hypothesis $F_2(t, \mathbf{r}_1, \mathbf{r}_2, \boldsymbol{\xi}_1, \boldsymbol{\xi}_2) = F_1(t, \mathbf{r}_1, \boldsymbol{\xi}_1)F_1(t, \mathbf{r}_2, \boldsymbol{\xi}_2)$ to obtain Eq. (2).

It is very interesting to consider a particular case of Liouville's equation (4) and of Bogolyubov's chain (5) that describe a spatially homogeneous gas consisting of a bounded number of particles and corresponding to two-particle collisions; in this case, on the final link of the chain, we obtain the Kac master equation [7]

$$\frac{\partial \varphi_1(t, \boldsymbol{\xi}_1)}{\partial t} = \frac{N-1}{N}\int [\varphi_2(t, \boldsymbol{\xi}_1', \boldsymbol{\xi}_2') - \varphi_2(t, \boldsymbol{\xi}_1, \boldsymbol{\xi}_2)] g_{12} d\sigma_{12} d\boldsymbol{\xi}_2, \tag{6}$$

where φ_1 and φ_2 are the one- and two-particle distribution functions. In contrast to the Boltzmann equation, Eq. (6) is linear, which will be used in the development and justification of efficient numerical direct statistical simulation schemes.

Returning to the Boltzmann equation, we easily obtain all the macroscopic parameters from the definition of the function f. For example, the number of molecules n in a unit volume of the gas is

$$n(t, \mathbf{r}) = \int f(t, \mathbf{r}, \boldsymbol{\xi}) d\boldsymbol{\xi}.$$

The mean velocity of the molecules, the strain tensor, and the energy flux are determined by the relations

$$\mathbf{V}(t, \mathbf{r}) = \frac{1}{n}\int \boldsymbol{\xi} f(t, \mathbf{r}, \boldsymbol{\xi}) d\boldsymbol{\xi},$$

$$P_{ij} = m\int c_i c_j f(t, \mathbf{r}, \boldsymbol{\xi}) d\boldsymbol{\xi},$$

$$q_i = \frac{m}{2}\int c^2 c_i f(t, \mathbf{r}, \boldsymbol{\xi}) d\boldsymbol{\xi},$$

where $\mathbf{c} = \boldsymbol{\xi} - \mathbf{V}$ is the thermal velocity of the molecules.

The mean energy of the heat motion of molecules is usually described in terms of the temperature

$$\frac{3}{2}kT = \frac{1}{n}\int \frac{mc^2}{2} f(t, \mathbf{r}, \boldsymbol{\xi}) d\boldsymbol{\xi}.$$

Applying the Chapman–Enskog procedure to the Boltzmann equation, we obtain the hydrodynamical level of description. This sequentially yields the Euler, Navier–Stokes, Barnett, etc., equations:

$$\frac{\partial \rho}{\partial t} + \frac{\partial \rho V_i}{\partial x_i} = 0,$$

$$\left(\frac{\partial}{\partial t} + V_j\frac{\partial}{\partial x_j}\right)V_i = -\frac{1}{\rho}\frac{\partial P_{ij}}{\partial x_j}, \tag{7}$$

$$\frac{3}{2}R\rho\left(\frac{\partial}{\partial t} + V_j\frac{\partial}{\partial x_j}\right)T = -\frac{\partial q_j}{\partial x_j} - P_{ij}\frac{\partial V_j}{\partial x_j},$$

$$P_{ij} = p_{ij} + \delta_{ij}p, \quad p = \rho RT, \quad p_{ij} = \mu\left(\frac{\partial V_i}{\partial x_j} + \frac{\partial V_j}{\partial x_i} - \frac{2}{3}\delta_{ij}\frac{\partial V_r}{\partial x_r}\right), \quad q_i = -\lambda\frac{\partial T}{\partial x_i}. \tag{8}$$

Following the general logic of the presentation, we may assume that the dynamics of continua, being a particular case of the kinetic treatment of the gas motion, has some statistical features; this fact will be used below.

3. CONSTRUCTION OF EFFICIENT STATISTICAL SIMULATION METHODS

The key role in rarefied gas dynamics is certainly played by the direct statistical simulation methods. The studies on the construction of the statistical procedures based on the direct simulation opened prospects for improving the efficiency of such methods by decreasing the computational cost and the required computer memory compared to the initial modifications of these methods. This made it possible to apply such methods for solving two-dimensional and then (with account for the actual properties of gases) three-dimensional problems. However, in the investigation and justification of these methods, it is impossible to do without the kinetic equation that describes the phenomenon being simulated. The establishment of the relationship of the statistical procedure with the solution to the kinetic equation is necessary for a number of reasons. First, this is important in order to be sure that the solution is correct and to enable one to use the results as a benchmark because many typical problems were first solved by the direct simulation methods. Second, the establishment of the correspondence between the simulation result and the solution makes it possible to use the well-developed techniques of regular numerical and statistical methods of solving the equations of mathematical physics for the analysis and improvement of the methods efficiency. Third, this makes it possible to form a general approach to the construction of the statistical methods and eliminates various incorrect modifications.

It must be stressed that the complexity of the practical problems of high altitude hypersonic aerodynamics requires the use of all the available theoretical, experimental, and numerical techniques developed for the investigation of rarefied gas flows. In this regard, the analysis of the kinetic equation and of its models becomes especially important. Various approximate representations of the collision integral and of the distribution function are often used. Among them, the most widespread approximations of the kinetic equation are the following ones.

(1) The model Krook equation (see [8])

$$\frac{df}{dt} = \nu(f_0 - f), \tag{9}$$

where ν is the frequency of collisions and $f_0 = n\left(\frac{m}{2\pi kT}\right)^{3/2}\exp\left(-\frac{m}{2kT}(\bar{\xi} - \bar{v})^2\right)$ is the equilibrium distribution function.

(2) The Holway ellipsoidal model

$$\frac{df}{dt} = \nu(f_e - f),$$

where f_e is the ellipsoidal distribution function.

(3) The approximation Shakhov model (see [9]), which, in contrast to the preceding models, yields the correct Prandtl number Pr:

$$\frac{df}{dt} = \nu(f^+ - f), \quad f^+ = f_0\left[1 + \frac{4}{5}(1 - \mathrm{Pr})s_\alpha c_\alpha\left(c^2 - \frac{5}{2}\right)\right], \quad s_i = \frac{1}{n}\int c_i c^2 f d\bar{\xi}, \tag{10}$$

where $\mathbf{c}$ is the dimensionless thermal molecular velocity.

(4) We also mention the linearized Boltzmann equation, which is rigorously derived from the complete Boltzmann equation under the condition that the distribution function is almost an equilibrium one:

$$\frac{d\varphi}{dt} = k(\bar{\xi})\varphi + \int L(\boldsymbol{\xi}, \boldsymbol{\xi}_1)\varphi_1 d\boldsymbol{\xi}_1.$$

Here, $f = f_0(1 + \varphi)$, $\varphi \ll 1$, and $k(\boldsymbol{\xi})$ and $L(\boldsymbol{\xi}, \boldsymbol{\xi}_1)$ are given functions of the molecular velocities depending on the kind of the particles.

The model equations, in contrast to the linearized equation, are not rigorously derived from the Boltzmann equation; moreover, they are much more nonlinear than the original equation. However, they can prove to be simpler in practical implementation.

From the practical point of view, the direct statistical simulation methods based on the Bird and Haviland approaches are naturally the most efficient, and their modifications have dominated the computational aerodynamics.

Presently, the leading place in rarefied gas dynamics is occupied by the Bird method; various modifications of this method developed by Russian researchers (see, e.g., [10–21]) improved the efficiency of the original method by several orders of magnitude. The idea of the method is to split the evolution of the system in a small interval of time into two physical processes:

(1) relaxation in accordance with the collision operator in the kinetic equation

$$\frac{\partial f}{\partial t} = J(f);$$

(2) free molecular transfer

$$\frac{\partial f}{\partial t} = -\boldsymbol{\xi}\nabla f.$$

This is the well-known first-order splitting scheme with respect to Δt for any operator equation. In this case, this approach is attractive because it splits the dynamics of a very complex kinetic system into two clear physical processes. The distribution function is modeled by N particles that first collide in each cell between themselves with a given frequency during the time Δt and then move at the distance $\boldsymbol{\xi}_j \Delta t$ during the time Δt.

The central role in the nonstationary statistical simulation method is played by the procedure used to count the collisions. A pair of particles is chosen for collision in accordance with the collision frequency independently of the distance between them in the given cell. The velocities of the particles after the collision are chosen according to the molecular interaction laws. Although the efficiency of the method depends on many parameters of the computation scheme (relaxation, splitting with respect to time, stabilization, time step, space grid, and so on), the main studies devoted to the improvement of the method focus on the improvement of the collision procedure and on reducing the statistical error because this is the main instrument that makes it possible to reduce the number of particles in the cells and thus decrease the computation time and the requirements for computer memory. For example, a modification of the collision procedure was proposed in [18] for a particular case of Maxwell's molecules. With this modification, the computation results are almost independent of the number of particles in a cell in the range from 40 to 6. (With the ordinary computation scheme, the number of particles in a cell must be about 30). In [11–16], a general method that is independent of the kind of molecules was proposed; in that method, the subsystem of particles in each cell is considered as an N-particle Kac model (6) at the stage of collisions.

The simulation of a collision is reduced to a statistical realization of the evolution of model (6) during the time Δt rather than to the realization of the Boltzmann equation (2). The collision time in the Kac model is calculated in accordance with collision statistics in the ideal gas following the Bernoulli scheme. This scheme makes it possible to use a considerably smaller number of particles in a cell and a finer grid. The analysis shows that the computation results are almost independent of the number of particles in a cell down to two particles. The point is that the Boltzmann equation requires the molecular chaos assumption to be satisfied; however, for the number of particles in a cell that can be processed by modern computers, this assumption is satisfied only with a systematic error. By contrast, Eq. (6) does not rely on this assumption; therefore, the collision is calculated as a Markov process. On the other hand, as $N \longrightarrow \infty$, the Kac model is completely equivalent to the spatially homogeneous Boltzmann equation. Thus, the approach developed by Belotserkovskii and Yanitskii provides a basis for constructing efficient numerical schemes for solving three-dimensional aerodynamic flow problems, and, on the other hand, it solves the important methodological problem of the equivalence of the numerical method and the solution of the kinetic equation.

A huge number of studies are devoted to the methods of the traditional use of statistical simulation. For this reason, we mainly consider aerodynamics problems in this paper. It has already been mentioned that the statistical methods are more efficient in practical problems of rarefied gas dynamics than the regular and semiregular methods. For the flow problems, which are the most important problems in aerodynamics, the statistical methods were successfully used for the calculation of aerodynamic characteristics of various (including very complex) bodies in free molecular and almost free molecular flows. The procedure, which was developed more than twenty years ago, is now implemented in standard computer programs and is widely used in many organizations. Applications in the case of smaller Knudsen numbers Kn present considerable computational difficulties due to the reduced mean free path of the molecules and, respectively, a finer step with respect to time and space; in the case of the direct statistical simulation; the number of particles that simulate the distribution function is also increased.

The method described above makes it possible to calculate the aerodynamic characteristics of real-life designs. Figures 1–4 show the characteristic shapes of hypersonic aircraft.

Figure 5 illustrates an example of the calculation of the aerodynamic characteristics of the hypersonic aircraft shown in Fig. 1 for various degrees of the gas rarefaction (the Reynolds number Re) and orientations (the angle of attack α).

4. LINEAR PROBLEMS OF COMPUTATIONAL AERODYNAMICS

Following [22], consider the flows that are close to the equilibrium flows. In this case, the distribution function can be written as

$$f = f_0(1 + \varphi), \quad \varphi \ll 1,$$

where

$$f_0 = n_0\left(\frac{m}{2\pi k T_0}\right)^{3/2} \exp\left(\frac{m}{2kT_0}\xi^2\right),$$

and the Boltzmann equation is linearized in the form

$$\mathbf{v}_x\frac{\partial\varphi}{\partial x} + \mathbf{v}_y\frac{\partial\varphi}{\partial y} + \mathbf{v}_z\frac{\partial\varphi}{\partial z} = -\varphi k(\mathbf{v}) + \int L(\mathbf{v}, \mathbf{v}_1)\varphi_1 d\mathbf{v}_1,$$

with $\mathbf{v} = \xi\sqrt{\frac{m}{2kT}}$.

The analytical expressions for the rigid sphere molecules have the form

$$k = a\int \mathbf{g}e^{-\mathrm{v}_1^2} d\mathbf{v}_1,$$

$$L = Be^{-\mathrm{v}^2}\left(\mathbf{g} - \frac{2}{\mathbf{g}}e^{\mathcal{D}^2}\right),$$

where $\mathbf{g} = \mathbf{v}_1 - \mathbf{v}$, and a and B are constant coefficients.

Integrating Eq. (11) along the trajectories, we obtain the linear integral equation

$$\varphi = \varphi_r + \int K\varphi_1 d\mathbf{v}_1 dl,$$

where

$$\varphi_r = \varphi_w \exp\left[-\frac{k}{\mathrm{v}}(\mathbf{l} - \mathbf{l}_0)\right],$$

$$K = \frac{1}{\mathbf{v}}L\exp\left[-\frac{k}{\mathrm{v}}(\mathbf{l}_1 - \mathbf{l}_0)\right].$$

The Ulam–Neumann statistical procedure is applicable to this equation (see [2]).

In the general case, the calculation by the Monte Carlo method is reduced to the evaluation of integrals. These integrals are expectations of the random variables used as estimates; in other words, a Lebesgue–

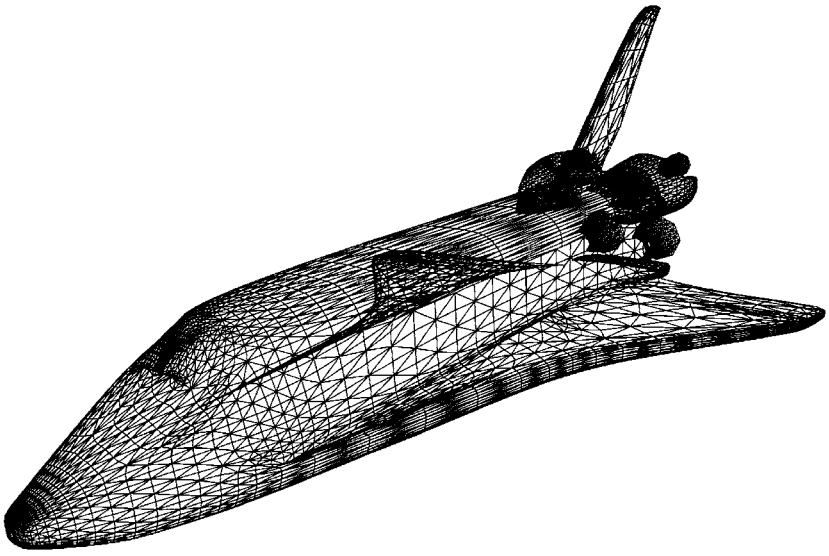

Fig. 1. The typical scheme of a space shuttle.

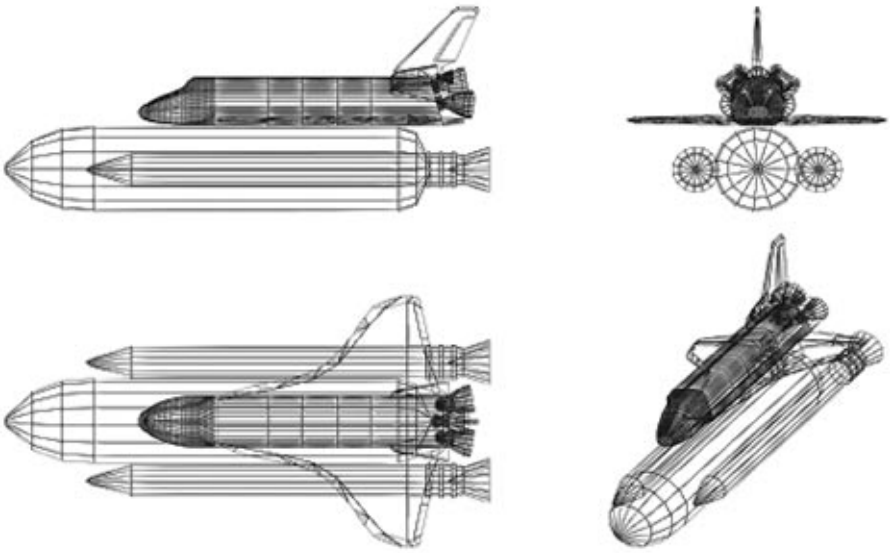

Fig. 2. The Energy–Buran system.

Stieltjes integral with respect to a certain probabilistic measure

$$\mathbf{I} = \int \psi(\mathbf{x})\mathbf{u}d\mathbf{x}$$

is evaluated using the arithmetic mean over the number of trials

$$\frac{1}{N}\sum_{i=1}^{N}\psi(x_i).$$

When integral equations are solved, the integral is a functional of the solution to the equation

$$\varphi(\mathbf{x}) = \varphi_r(\mathbf{x}) + \int K(\mathbf{x}, \mathbf{y})\varphi(\mathbf{y})d\mathbf{y},$$

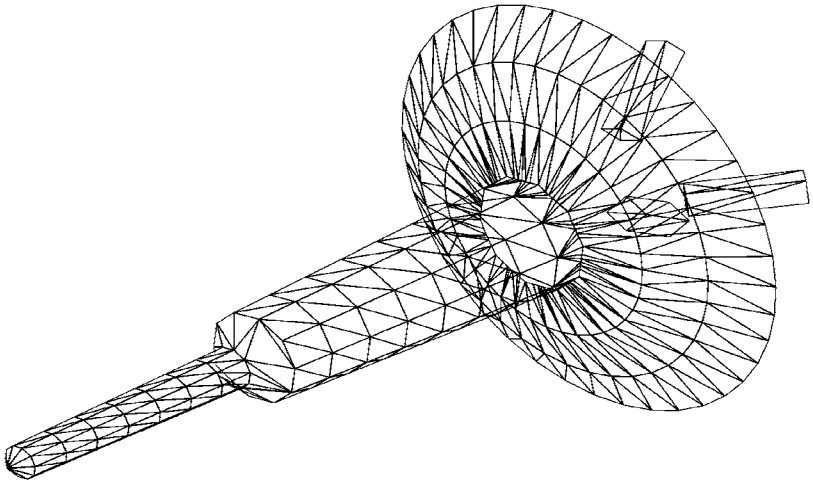

Fig. 3. A Martian probe.

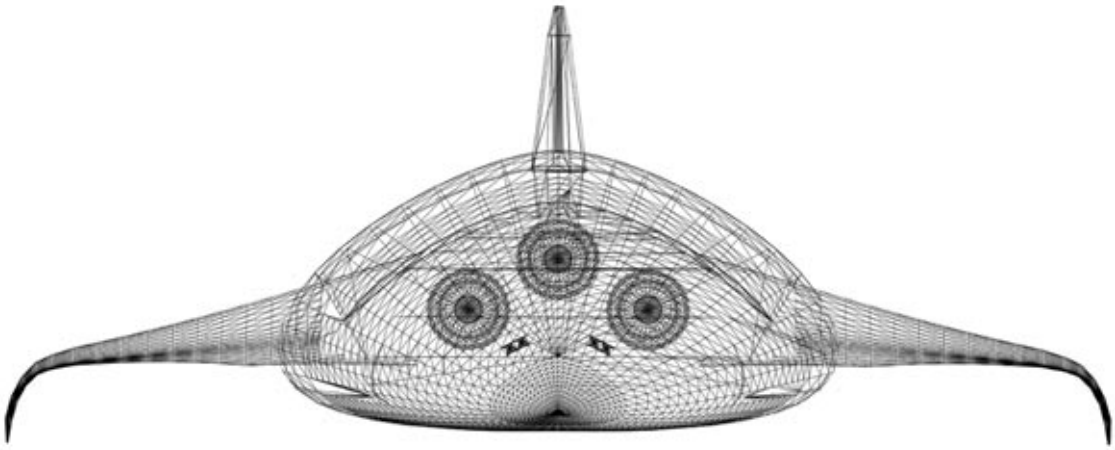

Fig. 4. A promising hypersonic aircraft.

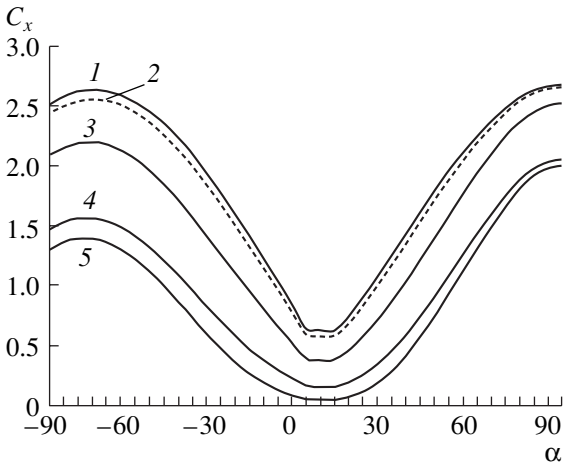

Fig. 5. (*1*) Free molecular flow, (*2*) transient mode (Re = 1), (*3*) transient mode (Re = 10), (*4*) transient mode (Re = 100), (*5*) continuous medium limit.

where $\mathcal{D}$ is a domain in the $\mathbb{S}$-dimensional Euclidean space, $x \in \mathcal{D}$, $y \in \mathcal{D}$; $\varphi(\mathbf{x})$ and $\varphi_r(\mathbf{x})$ are functions defined on $\mathcal{D}$; the kernel $K(\mathbf{x}, \mathbf{y})$ is defined on the Cartesian product of $\mathcal{D}$ by itself, and the integral in the equation is interpreted as the Lebesgue integral. The solution to such an equation is given by the converging Neumann series

$$\varphi(\mathbf{x}) = \sum_{i=0}^{\infty} \psi_i(\mathbf{x}),$$

where

$$\psi_i(\mathbf{x}) = \int_{\mathcal{D}} K(\mathbf{y}, \mathbf{x})\psi_{i-1}(\mathbf{y})d\mathbf{y}.$$

In this case, the unknown functional is represented as the sum of the multiple integrals

$$I = (\varphi, h) = \sum_{i=0}^{\infty} \int_{R_i} \varphi_r(\mathbf{x}_0)K(\mathbf{x}_0, \mathbf{x}_1)\ldots K(\mathbf{x}_{i-1}, \mathbf{x}_i)h(\mathbf{x}_i)d\theta_i,$$

where $R_i = \underbrace{\mathcal{D} \times \mathcal{D} \times \mathcal{D} \ldots \times \mathcal{D}}_{i}$, $R_0 = \mathcal{D}$, $d\theta_0 = d\mathbf{x}_0$, and $d\theta_i = d\mathbf{x}_0 \ldots d\mathbf{x}_i$.

Usually, a homogeneous Markov chain is assigned to the given integral equation. This chain is specified by the density of the initial distribution and the transition density $p(\mathbf{x} \longrightarrow \mathbf{y})$. The sample trajectory of this chain is constructed in accordance with the initial and the transition probability densities. Then, the estimate $\frac{1}{N}\sum_{i=1}^{N} \psi(\mathbf{x}_i)$ of the unknown functional has the form

$$\psi = \sum_{i=0}^{n} Q_i(\mathbf{x}_0, \ldots, \mathbf{x}_i)h(\mathbf{x}_i),$$

where

$$Q_0 = \frac{\varphi_r(\mathbf{x}_0)}{\pi(\mathbf{x}_0)}, \quad Q_i = Q_0 \frac{K(\mathbf{x}_0, \mathbf{x}_1)}{p(\mathbf{x}_0 \longrightarrow \mathbf{x}_1)} \cdots \frac{K(\mathbf{x}_{i-1}, \mathbf{x}_i)}{p(\mathbf{x}_{i-1} \longrightarrow \mathbf{x}_i)},$$

and n is the number of collisions in the trajectory.

Thus, given an analytical expression for the kernel, one can construct a simple algorithm for finding various functionals of the solution to the integral equation.

When the kinetic equation is solved numerically, the trajectories of the molecules (test particles) on the equilibrium distribution function are usually considered as a Markov chain. In this case, a simple realization of the trajectories that are close to the actual trajectoris is used, which significantly reduces the variance. The simulation process for a random variable is completely equivalent to the successive approximation method. Therefore, the solution obtained by the Monte Carlo method converges to the solution to the Boltzmann equation.

Figure 6 shows the solution to the linearized Boltzmann equation for the calculation of the diffusion coefficient of a Brownian particle and the comparison with Millikan's results.

5. POSSIBLE LINES OF DEVELOPMENT OF THE COMPUTATIONAL AERODYNAMICS METHODS

It has already been mentioned that presently the most popular methods are based on the Bird approach of simulation of an ensemble of molecules. However, some time ago the test particle statistical simulation methods based on the Haviland approach were prevailing. It is possible that in the future the efficiency of this approach will be improved or a new class of problems will appear for which this approach will be preferable. Even now there are some problems in physical chemistry for which the method is preferable. Also, this is the class of linear problems for which the test particle method was first proposed in [2]. The Haviland approach has one more advantage over the Bird method: for it, the problem of consistency with the solution to the kinetic equation is not so critical. As regards the computational aerodynamics, the Haviland method is based on the linearized Boltzmann equation (11).

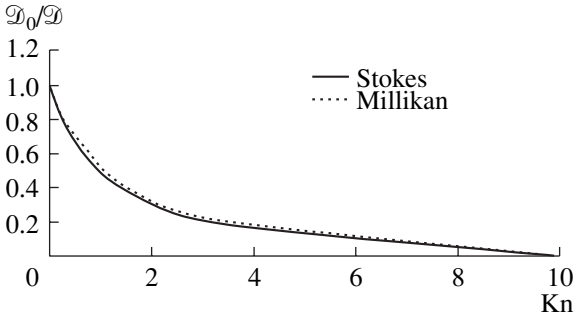

Fig. 6. The diffusion coefficient of a Brownian particle in a rarefied gas.

When developing the schemes of the stationary statistical simulation based on the Haviland test particle method, the process of solution can be considered as the solution of the Boltzmann equation

$$\boldsymbol{\xi}_1 \frac{\partial f}{\partial t} = \int (f' f_1' - f f_1) \mathbf{g} b db d\varepsilon d\boldsymbol{\xi}_1 = I - \nu f,$$

with

$$I = \int f_1' f' \sigma \mathbf{g} d\boldsymbol{\xi}_1, \quad \nu = \int f_1 \sigma g d\boldsymbol{\xi}_1,$$

in the integral form

$$f = f_w \exp\left(-\frac{1}{\xi}\int \nu dr\right) + \frac{1}{\xi}\int I \exp\left(-\int \nu dr\right) f d\mathbf{r},$$

where f_w is the boundary distribution function.

At each iteration step k, this equation written in the integral form

$$f^{(k+1)} = f_w \exp\left(-\int \nu^{(k)} dt\right) + \int \frac{I^{(k)}}{f^{(k)}} \exp\left(-\int \nu^{(k)} dt\right) f^{(k+1)} dt$$

is a linearized kinetic equation, which is solved by the Monte Carlo method using the Ulam–Neumann procedure described above.

At each iteration step, the macroparameters appearing in the original equation are calculated; these are n^{k+1}, u^{k+1}, T^{k+1}, and ν^{k+1}. Then, the next iteration is performed. If the successive approximation method is convergent, then the passage from one iteration to the next one finally yields a solution to the kinetic equation. The solution of mathematical equations and the direct simulation of the flows of rarefied gas are the traditional field of application of the Monte Carlo method. We consider the unconventional application of statistical simulation for solving problems concerning continuous media and turbulent flows.

6. THE DIRECT STATISTICAL SIMULATION METHOD FOR INVISCID IDEAL GAS FLOWS [23, 24]

The relationship between the kinetic and the continuous medium models can be illustrated using the direct statistical simulation (DSS) method for inviscid flows. The DSS methods for flows in a rarefied gas (Bird's approach) are based on the splitting of the evolution of a system of particles into two physical processes on the time interval Δt. These processes are described by the equations

$$\frac{\partial f}{\partial t} = I(f, f),$$

$$\frac{\partial f}{\partial t} + \xi_x \frac{\partial f}{\partial x} + \xi_y \frac{\partial f}{\partial y} + \xi_z \frac{\partial f}{\partial z} = 0.$$

They represent the change in the density of the distribution caused by the spatially homogeneous relaxation and the collision-free transfer, respectively. It is assumed that the time interval Δt is sufficiently small for

these processes to be considered as independent; Δt is of the order of magnitude of the mean free path, and the size of the cell is of the order of magnitude of the local mean free path.

When the deviation from the equilibrium state is small, the stage of the collision (relaxation) simulation can be replaced by a procedure of generating particle velocities in accordance with the given distribution. Inviscid flows can be modeled assuming that the result of relaxation in a cell is the establishment of an equilibrium distribution. The algorithm used to simulate the flows of an inviscid compressible ideal gas by the DSS method based on the use of the locally equilibrium distribution function f_0 consists of the following steps.

(1) Specification of the initial values of the macroparameters for each cell and the specification of the number of particles in each cell on the basis of the given statistics level depending on the volume of the cell.

(2) Distribution of the particles over the volume of the cell (specification of the coordinates).

(3) Generation of random velocities of the particles in the cell according to the mean velocity and the temperature on the basis of the distribution density f_0.

(4) Correction of the velocities to fully correspond to the mean values (the conservative property of the generation algorithm with respect to the momentum and energy).

(5)Simulation of the transfer of the particles in time Δt with the boundary conditions taken into account.

(6) Calculation of the macroparameters of the particles in the cells after the transfer.

(7) Repetition of Steps (2)–(6) up to a certain moment in time.

The initial values for the macroparameters are chosen using the conditions of the nonstationary problem or using an initial approximation for the solution of the stationary problem (Step 1).

The DSS method can be modified for inviscid flows so as to reduce the computational effort for the generation of particle velocities in each cell. Namely, once a set of velocities corresponding to the unit temperature and the zero mean velocity is generated, it can be then used for various mean velocities and temperatures in each cell. The procedure of the random distribution of the particles over the cell (Step 2) at each time step makes it possible to avoid the correlations that can appear when the same set of thermal velocities is used. Since the precalculated set of velocities is fixed and the actual number of particles in the cells is variable, weight coefficients are used to ensure the validity of the conservation laws.

The number of particles in a cell that is necessary for the simulation is determined in such a way that the statistical error

$$\delta \approx \sqrt{T}/\sqrt{N}$$

satisfies the error consistency condition $\delta \sim O(\Delta x, \Delta t)$. Here, N is the number of particles in the cell.

There is no need for tracing each particle during the entire calculation process because the distribution density is assumed to be given. The particles are traced individually only in the transfer process in order to count the macroparameters in the cells at the next time step.

The expressions for the components of the thermal velocity (Step 3) can be obtained by simulating the normally distributed random variable

$$\xi_x = \sqrt{\frac{2k_B T}{m}}\sqrt{-\ln\alpha_1}\cos(2\pi\alpha_2),$$

$$\xi_y = \sqrt{\frac{2k_B T}{m}}\sqrt{-\ln\alpha_1}\sin(2\pi\alpha_2),$$

$$\xi_z = \sqrt{\frac{2k_B T}{m}}\sqrt{-\ln\alpha_3}\cos(2\pi\alpha_4).$$

Here, α_k are independent random numbers that are uniformly distributed on the interval (0, 1). In order to reproduce the mean velocity more accurately, it is reasonable to use the following symmetrized algorithm: the thermal velocities of the particles with the odd indexes are calculated, and the thermal velocities of the particles with the even indexes are set equal to the velocities of the corresponding odd particles with the opposite sign.

Since the number of the modeled particles is bounded, the temperature of the generated set of velocities is slightly different from the temperature used to generate it. For this reason, a correction is required

(Step 4). Let us write the actual temperature of the generated set:

$$T_N = \frac{1}{3RN}\sum_{l=1}^{N}\xi_l^2.$$

Here, $R = k_B/m$ and N is the number of particles in a cell. Multiply the velocities by $\sqrt{T/T_N}$ to make the temperature equal to the given one. Then, all the conservativeness conditions are satisfied:

$$\frac{1}{N}\sum_{l=1}^{N}\xi_l = 0,$$

$$\frac{1}{3RN}\sum_{l=1}^{N}\xi_l^2 = T.$$

The coordinates of the particles at the step of the collision-free transfer (Step 5) are modified by the rule

$$\mathbf{r}_l^{t+\Delta t} = \mathbf{r}_l^t + \boldsymbol{\xi}_l^{t+\Delta t}\Delta t.$$

At this step, the particles are assigned the internal energies ε_l to take into account the internal degrees of freedom. When the particles are transferred, the boundary conditions must be satisfied. Concerning the rigid walls, it is assumed that the reflection of the particles is specular. It can be shown that this corresponds to the impermeability condition in the Euler equations. The conditions on the exterior boundaries through which the flow enters the domain and leaves it must correspond to the flow regime. Additional constraints can be taken into account, such as the condition that the fluxes of the mass, momentum, and energy are constant (the independency of these quantities of statistical fluctuations).

After the transfer step, the new values of the macroparameters in the cells are calculated with account for all the particles that arrived from the neighboring cells (Step 6):

$$\mathbf{V}^{t+\Delta t} = \frac{1}{N}\sum_{l=1}^{N}\boldsymbol{\xi}_l^{t+\Delta t},$$

$$T^{t+\Delta t} = \frac{2}{(3+\nu)k_B N}\sum_{l=1}^{N}\left\{\frac{m}{2}(\boldsymbol{\xi}_l^{t+\Delta t} - \mathbf{V}^{t+\Delta t})^2 + \varepsilon_l\right\}.$$

Under the local equilibrium condition, the internal degrees of freedom are taken into account by adding the term $\varepsilon_l = \nu k_B T'/2$, where T' is the temperature in the cell from which the particle arrived and ν is the number of the internal degrees of freedom. In such a system, the number of particles, the mean velocity, and the temperature are the working macroscopic variables.

The time step Δt is chosen from the condition that the particles belonging to the main group (i.e., the particles whose velocity differs from the macroscopic velocity (u, v, w) not greater than by the characteristic thermal velocity a) must be transferred not more than by a single cell:

$$\Delta t = CFL \times \min\left(\frac{\Delta x}{(|u|+a)}, \frac{\Delta y}{(|v|+a)}, \frac{\Delta z}{(|w|+a)}\right).$$

Here, a is the characteristic thermal velocity; e.g., $a = \sqrt{2RT} = c\sqrt{2/\gamma}$. It follows that $CFL \le 1$.

The scale of the mean free path is not used in this model; therefore, the space size of the cells is chosen in the same way as for the continuous media.

There is no clear stability condition for this method: if $CFL > 1$, then the particles can pass several cells, the algorithm remains the same, but its accuracy is lower. The condition imposed on Δt is an accuracy rather than a stability condition. The DSS method applied to inviscid flows is efficient in the regions of the flow in which the deviation from the equilibrium state is small. It reduces the computational cost of calculating the particle velocities after the collisions.

7. DESCRIPTION OF TURBULENT FLOWS: THE FLUID PARTICLES MODEL [16, 21]

By way of generalizing the application of kinetic models in mechanics of continua, an attempt was made to describe turbulent flows and, in particular, the dissipation of a turbulent spot. Here, as in rarefied gas dynamics, the problem is solved in terms of the distribution function. However, the pulsation of the velocity of a fluid particle $\mathbf{v}$ is used as an argument rather than the molecular velocity $\boldsymbol{\xi}$. It was Prandtl who first noticed a similarity between a rarefied gas and a turbulent fluid.

In Yanitskii's model, each particle in a cell has a new property (see table). As before, a fluid particle is characterized by its physical coordinates and its velocity. For the distribution density of the particles, a kinetic equation is proposed that is similar to the model equation in rarefied gas dynamics.

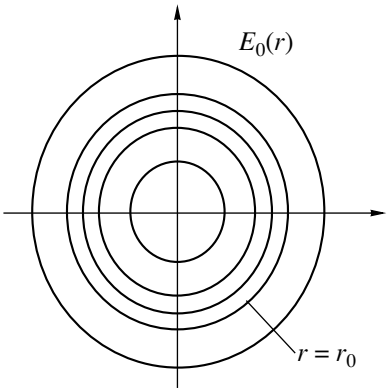

Fig. 7. Dissipation of the turbulent spot (the initial region).

The main purpose of such a consideration is to retain the main principles of the direct statistical simulation. To describe turbulence, the following Onufriev kinetic equation is used:

$$\frac{\partial f}{\partial t} + \mathbf{v}\frac{\partial f}{\partial \mathbf{x}} - \frac{1}{2\tau_1}\frac{\partial}{\partial \mathbf{v}}(\mathbf{v}'f) = \frac{f_M - f}{\tau_2}.$$

Here, $f_M = \left(\frac{3}{4\pi E}\right)^{3/2} \exp\left(-\frac{3\mathbf{v}'^2}{4E}\right)$ is the normal distribution and E is the turbulent energy density. This equation is similar to the Krook model equation.

The simulation scheme is organized according to the same principles as in rarefied gas dynamics. Fluid particles in the cells are considered, and the process is split into three steps: the convective transport

$$\mathbf{v}\frac{\partial f}{\partial \mathbf{x}},$$

the turbulent dissipation of energy

$$-\frac{1}{2\tau_1}\frac{\partial}{\partial \mathbf{v}}(\mathbf{v}'f),$$

and the redistribution of energy

$$\frac{f_M - f}{\tau_2}.$$

We numerically solved the spot dissipation problem in which the energy is initially concentrated in the region of radius r_0 (Fig. 7), the characteristic radius of the spot is $r_*(t)$, and the density of the turbulent energy is $E_m(t)$ at the center of the spot. The initial data are as follows:

$$f(0, r, \mathbf{v}) = f_0(r, \mathbf{v}),$$

$$E_0(r) = E_m^0 \exp\left(-\frac{r^2}{r_0^2}\right),$$

$$f_0(r, \mathbf{v}) = \left(\frac{3}{4\pi E_0}\right)^{3/2} \exp\left(-\frac{3\mathbf{v}'^2}{4E_0(r)}\right).$$

The numerical results are compared with the experimental ones in Fig. 8 ($\bar{r}_* = r_*(t)/r_0$ and $\bar{E}_m(t) = E/E_0$).

The kinetic models of turbulence (see Figs. 9, 10, and 11) are more informative because they describe the pulsations at the level of the distribution function. Such an approach to the description of turbulence seems to be promising because it makes it possible to take into account the large-scale turbulent process

Description of a media in terms of the distribution function

Rarefied gas dynamics	Turbulence
Particles	
Molecules	Fluid particles
$\mathbf{r}_i$—Molecule coordinates	$\mathbf{x}_i$—Particle coordinates
$\boldsymbol{\xi}_i$—Molecule velocities	$\mathbf{v}_i$—Pulsation velocities
Distribution function	
For molecules	For fluid particles
$f = f(t, \mathbf{r}, \boldsymbol{\xi})$	$f = f(t, \mathbf{x}, \mathbf{v})$
$\int f d\boldsymbol{\xi} = \rho$—density	$\int f d\mathbf{v} = 1$—normalization
Momenta	
$\int \boldsymbol{\xi} f d\boldsymbol{\xi} = \rho \mathbf{V}$—macroscopic velocity	$\int \mathbf{v} f d\mathbf{v} = \mathbf{V}$—mean velocity
$(\boldsymbol{\xi} - \mathbf{V})$—thermal velocity	$(\mathbf{v} - \mathbf{V})$—fluctuations

directly using the transport equation schemes and take into account the small-scale pulsations using the statistical simulation.

8. DESCRIPTION OF TURBULENCE USING THE THREE-WAVE RESONANCE MODEL [25]

Consider the Reynolds equation for the mean quantities U and V and the pulsations u, v, w, and p in the boundary layer approximation. Let d be the characteristic transversal scale of the flow and L be its longitudinal scale. When estimating the quantities in the original equations, the force characteristics are compared; therefore, $d \approx \delta^{**}$, where δ^{**} is the momentum thickness of the boundary layer. Hence, $\varepsilon^2 = d/L \ll 1$. Practically, $\varepsilon^2 \ll 10^{-2}$. Define

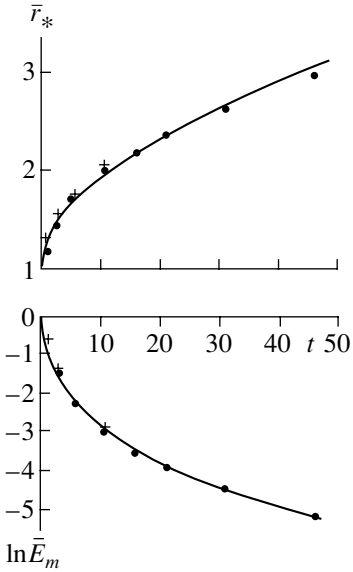

Fig. 8. Comparison of the direct statistical simulation (plus signs) with the Naudasher experimental data (dots).

$$\bar{u}_i = u_i/U_\infty, \quad \bar{x}_i = x_i/d, \quad i = 1, 2, 3,$$

$$\bar{t} = tU_\infty/d, \quad X = x/L, \quad T = tU_\infty/L,$$

$$\bar{U} = U/U_\infty, \quad \varepsilon^2 \bar{V} = V/V_\infty, \quad \varepsilon \bar{p} = p/\rho U_\infty^2,$$

$$\{u_i\} = (u, v, w), \quad \{x_i\} = (x, y, z).$$

Then, the equations for $\bar{U}$ and $\bar{V}$ have the form ($\mathrm{Re} = U_\infty d/\nu$)

$$\frac{\partial \bar{U}}{\partial T} + \bar{U}\frac{\partial \bar{U}}{\partial X} + \bar{V}\frac{\partial \bar{U}}{\partial \bar{y}} = -\frac{\partial \langle \overline{uv} \rangle}{\partial \bar{y}} + \frac{1}{\varepsilon^2 \mathrm{Re}}\frac{\partial^2 \bar{U}}{\partial \bar{y}^2},$$

$$\frac{\partial \bar{U}}{\partial X} + \frac{\partial \bar{V}}{\partial \bar{y}} = 0.$$

The equations for $\bar{u}_i$ and $\bar{p}$ have the form ($\mathrm{Re} = U_\infty \delta^{**}/\nu$)

$$\frac{\partial \bar{u}_i}{\partial \bar{t}} + \bar{U}\frac{\partial \bar{u}_i}{\partial \bar{x}_1} + f_i = -\frac{\partial \bar{p}}{\partial \bar{x}_i} + \frac{1}{\mathrm{Re}}\nabla^2 \bar{u}_i + \varepsilon T_i + O(\varepsilon^2),$$

$$\partial \bar{u}_i/\partial \bar{x}_i = 0.$$

In these equations, we use the notation

$$\{f_i\} = \left\{\bar{u}_2\frac{\partial \bar{U}}{\partial \bar{x}_1}, 0, 0\right\}, \quad T_i = \frac{\partial(\langle \bar{u}_i\bar{u}_j\rangle - \bar{u}_i\bar{u}_j)}{\partial \bar{x}_j}.$$

The boundary conditions are as follows: $\bar{u}_i(\bar{y} = 0; \infty) = 0$, $\bar{p}(\bar{y} = \infty) = 0$. It is assumed that $\mathrm{Re} \gg 1$ and $\varepsilon^2\mathrm{Re} \gg 1$.

Upon transforming the system to the equations for the vertical components of the velocity and of the vorticity and under the assumption that there is no resonance between the Tollmien–Schlichting and Squire waves, the equation for the vertical component of the vorticity can be dropped for simplicity. Expanding the vertical component of the velocity in the lower discrete spectrum of the Tollmien–Schlichting waves, we obtain

$$\frac{\partial a_{\bar{k}}}{\partial t} + i\left(\bar{\omega}(X_0, \bar{k}) - \frac{\partial \bar{R}_0}{\partial t}\bar{k}\right)a_{\bar{k}} - \varepsilon^2\frac{\partial}{\partial x}\left(\frac{\partial \bar{\omega}(X_0, \bar{k})}{\partial X_0}a_{\bar{k}}\right) = \varepsilon\int H_{\bar{k}\bar{k}'}a_{\bar{k}}a_{\bar{k}''}d\bar{k}' + \ldots,$$

$$\bar{k}'' = \bar{k} - \bar{k}',$$

where $k = \bar{k} = (\alpha, \beta)$, $\bar{\omega}(X_0, \bar{k})$, and $\bar{R}_0 = (X_0, Z_0)$ are, respectively, the dimensionless wave vector, the eigenvalues of the Orr–Sommerfeld equation, and the "center of mass" of the coordinates of the wave packet. The amplitudes $a_{\bar{k}}$ are related to the vertical velocity of the perturbation $v(x, y, z)$ by

$$v_{\bar{k}}(y) = a_{\bar{k}}\frac{v_0(y)}{N} + \ldots,$$

$$N = -\int_0^\infty\left(\frac{d\hat{v}_0(y)}{dy}\frac{dv_0(y)}{dy} + k^2\hat{v}_0(y)v_0(y)\right)dy,$$

where $v_0(y)$ is the lower Tollmien–Schlichting mode, $\hat{v}_0(y)$ is the eigenfunction, and $v_{\bar{k}}(y)$ is the Fourier image of $v(x, y, z)$.

Under certain assumptions, the "density" of the wave packets $I(\bar{k}) = \dfrac{\langle a^*_{\bar{k}}a_{\bar{k}?}\rangle}{\delta(\bar{k} - \bar{k}')}$ satisfies the transport equation

$$\frac{\partial I(\bar{k})}{\partial T} + g(\bar{k}, X)\frac{\partial I(\bar{k})}{\partial X} - h(\bar{k}, X)\frac{\partial I(\bar{k})}{\partial \bar{k}} - 2\bar{\omega}^I I(\bar{k}) = J_C,$$

$$g(\bar{k}, X) = \frac{\partial \bar{\omega}^R(\bar{k}, X)}{\partial \alpha},$$

$$h(\bar{k}, X) = \frac{\partial \bar{\omega}^R(\bar{k}, X)}{\partial X}.$$

This equation resembles the kinetic equation and describes the birth of quasiparticles in the region of instability of the Tollmien–Schlichting lower mode, their motion with the group velocity $g(\bar{k}, X)$ under the influence of the "force" $-h(\bar{k}, X)$, and the disintegration and the fusion of the particles caused by the three-wave resonance described by the term J_C. In the elementary case, the collision integral of this type is written as

$$J_C = \int d\bar{k}_1 P(\bar{k}, \bar{k}_1)\delta[\bar{\omega}^R(\bar{k}) - \bar{\omega}^R(\bar{k}_1) - \bar{\omega}^R(\bar{k}_2)][I(\bar{k}_1)I(\bar{k}_2) - I(\bar{k})I(\bar{k}_1) - I(\bar{k})I(\bar{k}_2)],$$

$$\bar{k} = \bar{k}_1 + \bar{k}_2.$$

To investigate the equation for the wave packet $I(\bar{k})$, which is similar to the kinetic equation, the direct statistical simulation method can be used, which proved to be efficient for simulating the phenomena described by kinetic equations.

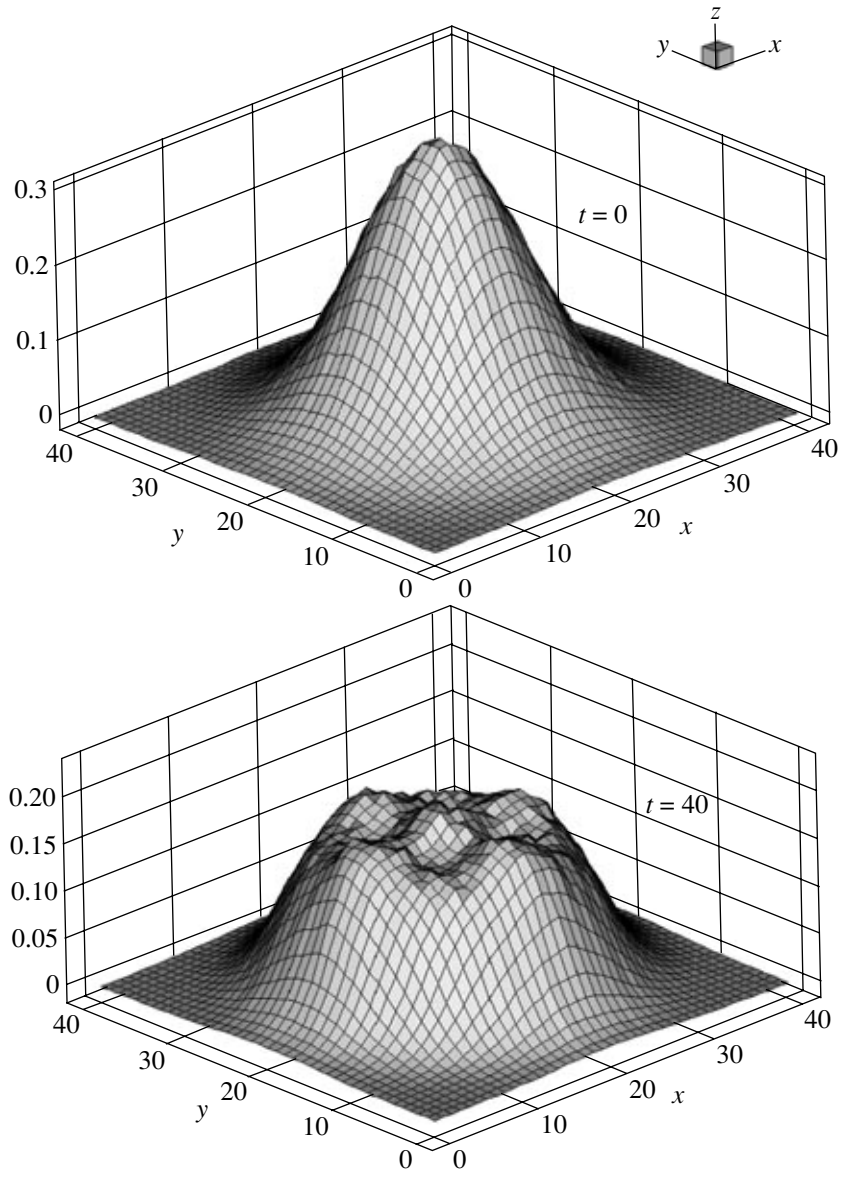

Fig. 9. Distribution of the specific energy in a turbulent spot.

For example, the following procedure for the direct statistical (Monte Carlo) simulation can be used. We will seek a solution $I(\bar{k})$ to the equation on the interval Δt assuming that it is sufficiently small. A discretization of the equation for $I(\bar{k})$ can be written as

$$I_{\bar{k}}(t+\Delta t) = I_{\bar{k}}(t)(1 - A_{\bar{k}}\Delta t) + A_{\bar{k}}\Delta t(\gamma'_{\bar{k}} + \int k' I_{\bar{k}_1} I_{\bar{k}_2} d\bar{k}_1),$$

$$A_{\bar{k}} = \int V_{\bar{k}\bar{k}_1\bar{k}_2}(I_{\bar{k}_1} + I_{\bar{k}_2})d\bar{k}_1,$$

$$k_{\bar{k}\bar{k}_1\bar{k}_2} = V_{\bar{k}\bar{k}_1\bar{k}_2}\delta[\omega^R(\bar{k}) - \omega^R(k_1) - \omega^R(k_2)],$$

$$k' = k_{\bar{k}\bar{k}_1\bar{k}_2}/A_{\bar{k}},$$

$$\gamma'_{\bar{k}} = \gamma_{\bar{k}}/A.$$

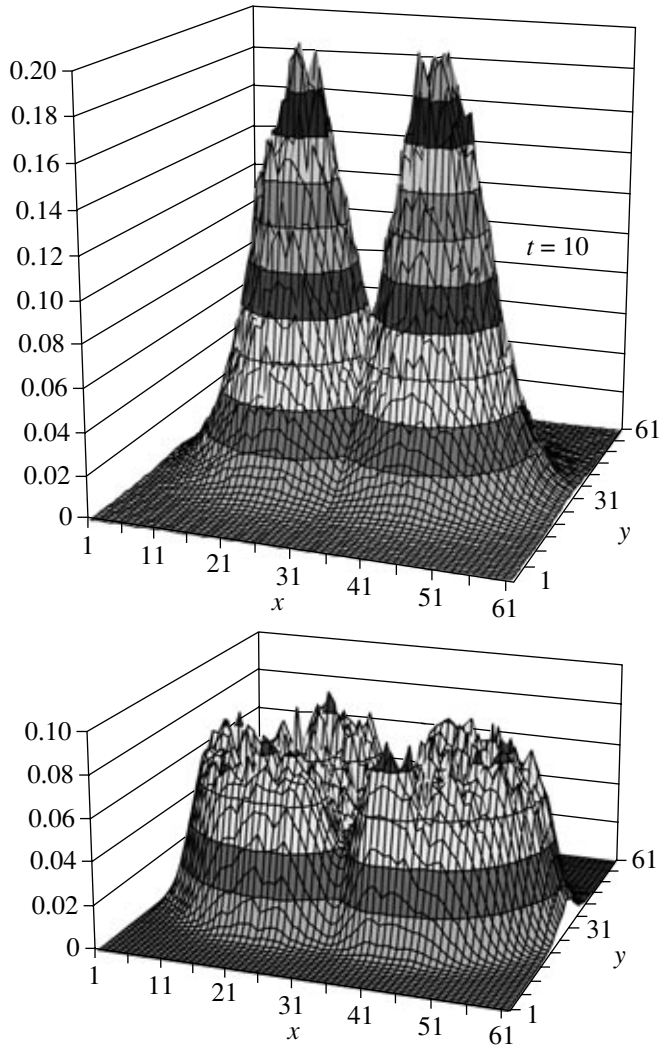

Fig. 10. The distribution of the turbulent energy of interacting spots.

Let us consider the function $I(\bar{k})$ as the density of some particles in the space of the vectors $\bar{k}$. In the course of time, this density changes, and the relationship between the density at the time t and the time $t + \Delta t$ is described by the equation under consideration.

Since we assume that $I(\bar{k})$ is known at the time t, the quantities $A_{\bar{k}}$, $\gamma'_{\bar{k}}$, and k' are also known. If we choose Δt such that $A_{\bar{k}}\Delta t < 1$, then we can use the superposition principle; i.e., at the time $t + \Delta t$, the density is equal to $I_{\bar{k}}(t)$ with the probability $(1 - A_{\bar{k}}\Delta t)$ and it is equal to $\gamma'_{\bar{k}} + \int k' I_{\bar{k}_1} I_{\bar{k}_2} d\bar{k}_1$ with the probability $A_{\bar{k}}\Delta t$. If this density at the time t is modeled by a certain number of particles (at the initial moment, the number of particles can be zero), then these particles do not change their coordinates with the probability $(1 - A_{\bar{k}}\Delta t)$; and, with the probability $A_{\bar{k}}\Delta t$, either new particles are born with the frequency k' or the coordinates of the particles change with the frequency $\gamma'_{\bar{k}}$. The expression related to the birth of the particles can be considered as the superposition

$$\gamma'_{\bar{k}} + \int k' I_{\bar{k}_1} I_{\bar{k}_2} d\bar{k}_1 = C_1 \gamma'_{\bar{k}} + C_2 \int k' I_{\bar{k}_1} I_{\bar{k}_2} d\bar{k}_1,$$

$$C_1 = \frac{1}{C}\int \gamma'_{\bar{k}} d\bar{k}, \quad C_2 = \frac{1}{C}\int k' I_{\bar{k}_1} I_{\bar{k}_2} d\bar{k} d\bar{k}_1,$$

$$C = C_1 + C_2.$$

Algorithm 1 ($I_k(t + \Delta t)$ Calculations)

Step 1. In the space of the vectors $\bar{k}$, the coordinates of a certain number of particles are specified in accordance with the initial density (which can be equal to zero; in that case, there are no particles in the space at the initial moment).

Step 2. $A_{\bar{k}}$, k', and $\gamma'_{\bar{k}}$ are calculated. If it turns out that $A_{\bar{k}}\Delta t > 1$, then Δt is modified.

Step 3. The field is not changed with the probability $(1 - A_{\bar{k}}\Delta t)$. Then, the corresponding macroparameters are calculated and the calculation proceeds to Step 4.2.

Step 4. With the probability $A_{\bar{k}}\Delta t$, new particles are born.

4.1. With the probability C_1, new particles are born with the density $\gamma'_{\bar{k}}$.

4.2. With the probability C_2, the particles in the field change their coordinates.

4.3. Having reached the boundary of the computation domain, the particles disappear.

Step 5. Upon calculating the macroparameters, the calculation proceeds to the next step.

9. SIMULATION OF THE EVOLUTION OF A VORTICITY SYSTEM IN A RAREFIED GAS [26–28]

An important problem in turbulence theory is finding the spectrum of the energy in a turbulent flow because this is the main characteristic of the turbulence. It is known that the size of small vortexes in turbulent flows can exceed the mean free path only by 2 or 3 orders of magnitude. Therefore, the investigation of the cascade vorticity phenomena in rarefied gases is important. The simulation of flows for small values of the Knudsen number makes it possible to examine the transition regimes that are close to a continuum medium but still have essential differences from it.

Consider the two-dimensional problem concerning the evolution of a vorticity system in a rarefied gas in the transition regime with the Knudsen number 0.01 subject to the special Taylor–Green initial conditions and periodic boundary conditions. When the initial flow field evolves in the course of time, small vortexes separate from the large ones, which is one of the main features of turbulent flows. This problem makes it possible to examine the evolution of the initial vortex structure at the kinetic level and to examine the transfer of energy to a smaller scale with the subsequent dissipation of the kinetic energy into heat. To solve this problem, we used the direct statistical simulation method with the relaxation algorithm corresponding to the Boltzmann collision integral.

As the main characteristics of the evolution of a vortex cascade, we used the distribution of the flow parameters at the sequential moments of time and the distribution of the spectral density of the energy over the wave numbers. The last characteristic can be compared both with the theoretical and experimental results for the inertial range in turbulent flows.

At $t = 0$, the following distributions of the density, the velocity components, and the temperature are specified:

$$u_0(x, y) = A\sin(2\pi x)\cos(2\pi y),$$

$$v_0(x, y) = B\cos(2\pi x)\sin(2\pi y),$$

$$\rho_0(x, y) = 1 + C\sin(2\pi x)\sin(2\pi y),$$

$$T_0(x, y) = 1 + D\cos(2\pi x)\cos(2\pi y).$$

Here, $A = 0.5$, $B = -0.4$, and $C = D = 0.1$. On the exterior boundaries, the following periodic boundary conditions are specified: $F(x + 1, y + 1, z + 1) = F(x, y, z)$, $0 < x < 1$, $0 < y < 1$, and $0 < z < 1$. The initial conditions correspond to the subsonic case, $M_{max} = 0.39$ is the maximal Mach number determined for the initial field, $\gamma = 5/3$ is the specific heat ratio for monoatomic gases, Kn = 0.01 is the Knudsen number, and Re = M_{max}/Kn = 39 is the Reynolds number.

The computation domain in which the evolution of the system of particles is examined is a cube of the size $L_x \times L_y \times L_z = 1 \times 1 \times 1$. A uniform grid of the size $110 \times 110 \times 1$ was used. This size is determined from

the value of the local Knudsen number. The size of the cells is determined depending on the mean free path: $\Delta x \le \lambda_{\min}$. In order to satisfy the boundary conditions, the coordinates of the particles that cross the domain boundary are recalculated.

For each computational realization, $N = 75$ particles were placed in each cell assuming that the density is equal to unity. 416 realization were performed so that the total number of particles was 31200.

For comparison, computations for the Euler equations were performed using a difference scheme of the second-order of accuracy with respect to the space variables and the time (the TVD approach and the Runge–Kutta method). The size of the computation grid was 200×200 cells.

Algorithm 2 (of simulating the spatially homogeneous relaxation on the basis of the majorant frequency scheme)

Step 1. The initial values of the macroparameters are specified in the cells, and the number of particles in each cell is determined according to the density and the size of the cell using the given level of statistics, and the distribution of the particles in the cell (i.e., the specification of their initial coordinates and the generation of the particle velocities in accordance with the mean velocity and the temperature on the basis of the initial equilibrium distribution function f_0).

Step 2. Realization of the homogeneous relaxation process in the cells using the majorant frequency scheme.

Step 3. Transfer of the particles in the time Δt.

Step 4. Recalculations to meet the boundary conditions.

Step 5. Calculation of the macroparameters in the cells after the collisions and particle transfer.

Step 6. Repeat steps 2–6 up to a certain moment in time.

The numerical implementation of the collision relaxation in a subsystem consisting of N particles in a cell based on the majorant frequency scheme assumes that a correct estimate of the majorant ν_m of the collision frequency $\nu(\mathbf{C})$, where $\mathbf{C} = \{\boldsymbol{\xi}_1, \ldots, \boldsymbol{\xi}_N\}$, i.e., $\nu(\mathbf{C}) \le \nu_m$, is found; and the time transition in the Markov chain is realized according to the collision frequency ν_m. When the collisions are realized, dummy collisions with the frequency $\nu_m - \nu(\mathbf{C})$ are introduced such that the particle velocities do not change as a result of these collisions. This principle of constructing the Markov chain is known as the maximal section method; it is used in the Monte Carlo methods. In the process of simulation, the actual collisions occur with the frequency $\nu(\mathbf{C})/\nu_m$. In the implementation of this algorithm, there is no need for the calculation of $\nu(\mathbf{C})$ for each collision; it is sufficient to know the quantity $\max[g\sigma(g)]$, where $\sigma(g)$ is the total section of the collisions. Only the models of the intermolecular interactions for which $\nu(\mathbf{C}) < \infty$ are considered. Therefore, a majorant ν_m for $\nu(\mathbf{C})$ can always be found.

The collision frequency in a cell can be written as

$$\nu(\mathbf{C}) = \frac{N}{2} n \langle \sigma g \rangle,$$

where $n = (N-1)/V$ is the numerical density, N is the number of particles in the cell, and V is the volume of the cell. For the rigid sphere model, which we use, $\sigma(g) = \sigma = \text{const}$, the mean free path is $\lambda = 1/(n\sigma)$, $\mathrm{Kn}_l = \mathrm{Kn}/\rho = \lambda/L$, Kn_l is the local Knudsen number for the cell, Kn is the specified Knudsen number, ρ is the dimensionless density, and L is the characteristic size of the domain. Then, $\nu_m = \frac{1}{2} N g_{\max}/\lambda = \frac{1}{2} N g_{\max}/(L\mathrm{Kn}_l)$.

The reasonable value $g_{\max} \approx \sqrt{RT}$ should be used in the calculations.

In the framework of the majorant frequency scheme, the time separating the next collision from the preceding one in the sequence of collisions within the time interval Δt is realized according to the Poisson distribution with the frequency ν_m:

$$\tau = -(\nu_m)^{-1} \ln \alpha.$$

Here, α is an independent random number uniformly distributed on the interval (0, 1). The quantity τ is added to the time counter; if $\Sigma\tau \le \Delta t$, the collision is simulated; namely, a pair of particles with the velocities $(\boldsymbol{\xi}_i, \boldsymbol{\xi}_j)$ is uniformly chosen from $N(N-1)/2$ pairs and, if the condition

$$g_{ij}/g_{\max} > \beta,$$

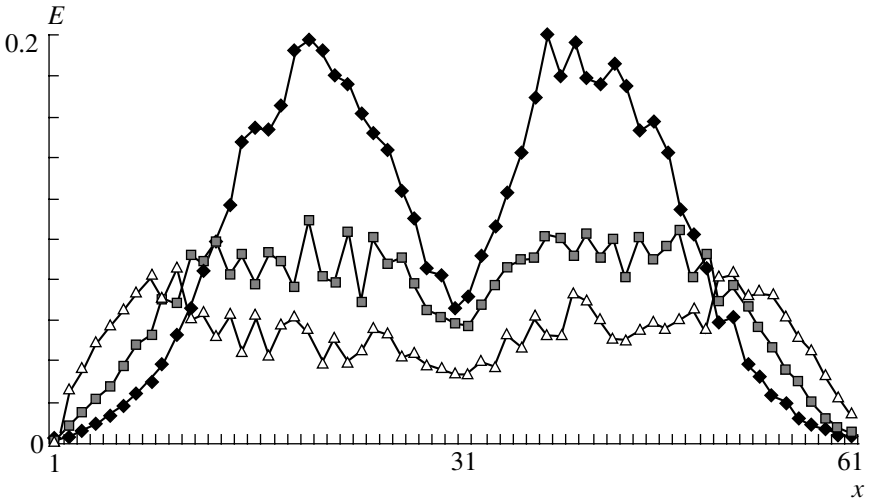

Fig. 11. The interaction of two turbulent spots (the cross section at $y = 31$, ◆ for $T = 0$, ■ for $T = 20$, and △ for $T = 40$).

where β is an independent random number uniformly distributed on the interval (0, 1), the velocities of the particles after the collision are calculated using the conservation laws; otherwise, the collision is considered as a dummy one and the particle velocities are not changed. If $g_{ij} > g_{\max}$, then we set $g_{\max} = g_{ij}$ and recalculate the collision.

The particle velocities are found by the rules

$$\boldsymbol{\xi}_i = \boldsymbol{\xi}_c + \frac{1}{2}\mathbf{g}', \quad \boldsymbol{\xi}_j = \boldsymbol{\xi}_c - \frac{1}{2}\mathbf{g}',$$

where $\boldsymbol{\xi}_c = (\boldsymbol{\xi}_i + \boldsymbol{\xi}_j)/2$ is the velocity of the center of mass of the pair of particles. In the framework of the rigid sphere model, the direction of the vector $\mathbf{g}'$ after the collision is isotropic; therefore, $\bar{\mathbf{g}}'$ can be efficiently determined with regard for the fact that $g' = g$:

$$g'_x = g\sin\theta\cos\varphi, \quad g'_y = g\sin\theta\sin\varphi, \quad g'_z = g\cos\theta.$$

Here, $0 \le \theta \le \pi$ and $0 \le \varphi \le 2\pi$ are the uniformly distributed angles.

At the transfer step, the coordinates of the particles are modified by the rule

$$\mathbf{r}^{t+\Delta t} = \mathbf{r}^t + \boldsymbol{\xi}^{t+\Delta t}\Delta t,$$

and each particle in the system moves at the distance proportional to its velocity.

The boundary conditions are satisfied by a periodic transfer when a particle crosses the boundary.

The majorant frequency scheme is an exact implementation of the DSS method for the main kinetic equation describing the step of the spatially homogeneous relaxation.

From the viewpoint of the computational effort, the accuracy of the results obtained using the DSS method is mainly determined by the total statistical ensemble obtained after a certain number of independent realizations; moreover, the algorithm based on this method is easily parallelized for multiprocessors.

The characteristics of the vorticity system determined by the given initial conditions are considered at the successive moments $t = 0.1$ and $t = 0.2$. Figure 12 shows the distribution of the density at these moments (on the left). The data for the limit case in the framework of the Euler equations are presented on the right.

The successive distributions of the density indicate the evolution of a system of vortexes. Although the simulation time corresponds to the initial phase of the process, the appearance of new scales is observed. The patterns of the distribution of the parameters in both cases (the rarefied gas and the continuous medium) are very similar to each other. This supports the claim that the dynamics of large vortexes can be described in short intervals of time in the framework of the Euler model. However, this is not true for smaller scales, which dissipate more strongly.

The construction of the spectrum of the kinetic energy of the flow $E(k)$ with respect to the wave numbers $k = |\mathbf{k}|$, where $\mathbf{k}$ is the wave vector, is a difficult problem. The spectral density of the kinetic energy for an isotropic turbulent flow in the two-dimensional case is given by

$$E(k) = E(\mathbf{k})/(2\pi k),$$

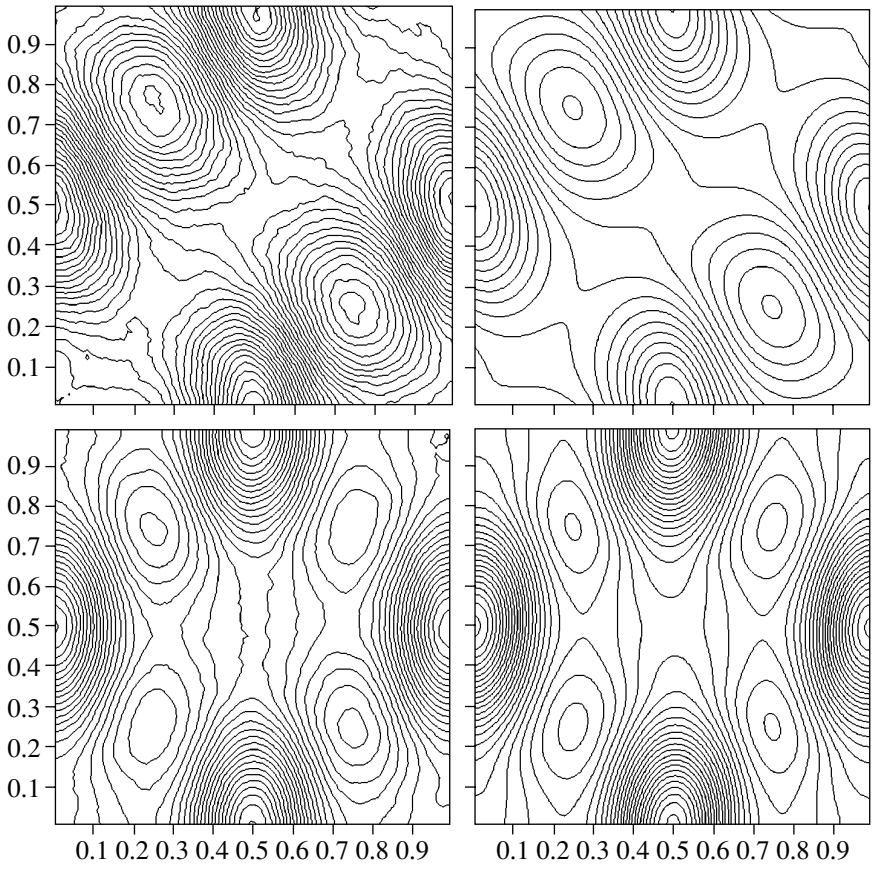

Fig. 12.

where $E(\mathbf{k})$ is the multidimensional spectral density of the kinetic energy. The complexity of the problem is in the fact that the calculation data are perturbed by the statistical fluctuations; for this reason, the Fourier transform can yield incorrect values of the amplitudes in the region of the wave numbers corresponding to the dissipative scales. One possible way of solving this problem is to find the Fourier coefficients using the least-squares method. Having found the Fourier coefficients of the expansion of the spatial distribution of the kinetic energy, we find the amplitudes E_k corresponding to the wave numbers k:

$$E = \sum_k a_k \sin(kx) + b_k \cos(kx), \quad E_k = \sqrt{a_k^2 + b_k^2}.$$

Under the isotropic turbulence assumption, the characteristics of the Fourier spectra of the random fields are invariant under the rotations of the wave vector; therefore, the spectrum can be found from a single direction of the wave vector. It should be noted that, for small Reynolds numbers, the isotropy assumption is not quite correct because the spectrum of the vortex scales is not broad enough. For this reason, when analyzing the computation results, some representative directions were chosen and the results were averaged.

Figure 13 shows the distribution of the spectral density of the kinetic energy at a finite time obtained using the DSS method (dots) and using the finite difference method for the

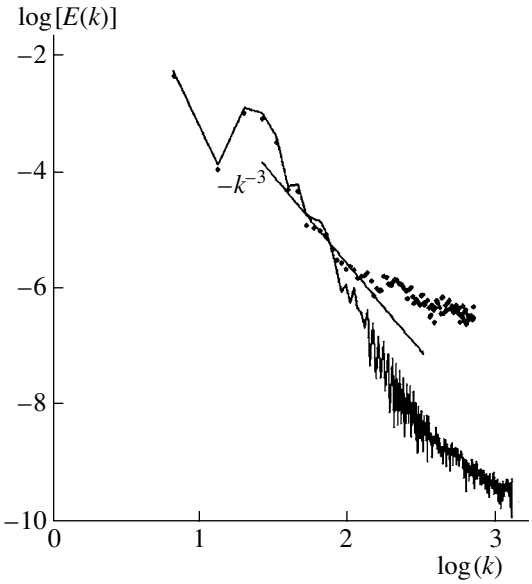

Fig. 13.

Euler equations (the solid curve). The spectrum indicates that the main part of the energy is concentrated in large vortexes. One can distinguish the interval of wave numbers in which the spectrum has the slope –3, which corresponds to the inertial interval of transferring the energy from small wave numbers to large ones under the assumptions of the qualitative turbulence theory in the two-dimensional case. Due to the small value of the Reynolds number, this flow cannot be classified as a well-developed turbulent flow: the range of scales in which the formation of the inertial interval can be expected is too small, and the result has a qualitative nature. The spectrum obtained on the basis of the Euler equation is consistent with the spectrum for a rarefied gas in the region of large scales up to $\log(k) = 1.7$; then, it rapidly decays. The presence of the interval with the slope of the spectral curve equal to –1 in the region of large wave numbers ($\log(k) > 2.25$) is explained by the fluctuations obtained in the process of the statistical simulation.

The data indicating the existence of an inertial interval are consistent with the results obtained in [29], where the same problem was solved using the discrete velocity method and in the framework of other kinetic approaches. It is important that there is experimental evidence supporting the same spectral dependence for almost two-dimensional flows in thin films (see [26]).

ACKNOWLEDGMENTS

This work was supported by the Russian Foundation for Basic Research (project no. 04-07-90345-c) and by the Leading Scientific Schools Program (project no. 96-15-96063).

REFERENCES

1. A. Hall, "On An Experimental Determination of π," Messeng. Math, No. 2, 113–114 (1873).
2. N. Metropolis and S. Ulam, "The Monte-Carlo Method," J. Amer. Stat. Assoc. **44** (247), 335–341 (1949).
3. V. S. Vladimirov and I. M. Sobol', "Calculation of the Minimal Eigenvalue of the Peierls Equation by the Monte Carlo Method," in *Computational Mathematics and Mathematical Physics* (Akad. Nauk SSSR, Moscow, 1958), No. 3, pp. 130–137 [in Russian].
4. J. K. Haviland and M. D. Lavin, "Application of the Monte-Carlo Method to Heat Transfer in Rarefied Gases," Phys. Fluids **5** (1), 279–286 (1962).
5. G. A. Bird, "Shock-Wave Structure in Rigid Sphere Gas" in *Rarefied Gas Dynamics* (Academic, New York, 1965), Vol. 1, pp. 25–31.
6. S. M. Ermakov, *Monte Carlo Method and Related Topics* (Nauka, Moscow, 1985) [in Russian].
7. M. Kac, *Probability and Related Topics in Physical Sciences* (New York, 1957; Mir, Moscow, 1965) [in Russian].
8. P. L. Bhathnagar, E. P. Gross, and M. Krook, "A Model for Collision Processes in Gases. I. Small Amplitude Processes in Charged and Neutral One-Component Systems," Phys. Rev. **94** (3), 511–525 (1954).
9. Yu. I. Khlopkov and E. M. Shakhov, "Kinetic Models and Their Role in the Investigation of Flows in Rarefied Gas," in *Numerical Methods in the Dynamics of Rarefied Gas* (Vychisl. Tsentr Akad. Nauk SSSR, Moscow, 1972), No. 3, pp. 34–80 [in Russian].
10. V. E. Yanitskii, "A Statistical Model of the Flows in an Ideal Gas and Its Features," in *Numerical Methods in Mechanics of Continua* (SO AN SSSR, Novosibirsk, 1975), Vol. 6, No. 4, pp. 139–150 [in Russian].
11. O. M. Belotserkovskii and V. E. Yanitskii, "The Statistical Method of Particles in Cells in Rarefied Gas Dynamics, Part I," Zh. Vychisl. Mat. Mat. Fiz. **15**, 1195–1208 (1975).
12. O. M. Belotserkovskii, "Computational Experiment: The Direct Numerical Simulation of Complex Flows in Gas Dynamics Based on the Euler, Navier–Stokes, and Boltzmann Equations," in *Karman Lecture* (Institute of Fluid Dynamics, Brussels, 1976).
13. O. M. Belotserkovskii and V. E. Yanitskii, "Numerical Methods in Rarefied Gas Dynamics," in *Proc. of the IV All-Union Conference on Rarefied Gas Dynamics* (Tsentral'nyi Aerogidrodinamicheskii Institut, Moscow, 1977), pp. 101–183 [in Russian].
14. O. M. Belotserkovskii and V. E. Yanitskii, "The Statistical Method of Particles in Cells in Rarefied Gas Dynamics, Part II," Zh. Vychisl. Mat. Mat. Fiz. **15**, 1553–1567 (1975).
15. O. M. Belotserkovskii and V. E. Yanitskii, "Numerical Simulation of Flows in Rarefied Gas," Usp. Mekh. **1** (1–2), 69–112 (1978).
16. O. M. Belotserkovskii, *Numerical Simulation in Mechanics of Continua* (Nauka, Moscow, 1984) [in Russian].
17. V. I. Vlasov, "Calculation of a Rarefied Gas Flow around a Plate at an Angle of Attack," Uchenyi Zapiski Tsentr. Aerogidrodinamicheskogo Inst. **4** (1), 17–24 (1973).
18. S. L. Gorelov and A. I. Erofeev, "Influence of Internal Degrees of Freedom on a Hypersonic Rarefied Gas Flow around a Plate," Izv. Akad. Nauk SSSR, Ser. Mekhan. Zhidk. Gaza, No. 6, 151–156 (1979).
19. O. M. Belotserkovskii, A. I. Erofeev, and V. E. Yanitskii, "On the Time-Dependant Direct Statistical Simulation Method for Rarefied Gas Flows," Zh. Vychisl. Mat. Mat. Fiz. **20**, 1174–1204 (1975).

20. O. M. Belotserkovskii, A. I. Erofeev, and V. E. Yanitskii, *Direct Statistical Simulation in Aerodynamics* (Vychisl. Tsentr Akad. Nauk SSSR, Moscow, 1983) [in Russian].
21. O. M. Belotserkovsky, A. I. Yerofeev, and V. E. Yanitsky, "Direct Monte-Carlo Simulation of Aerohydrodynamics Problems," in *Proc. XIII Int. Symp. on Rarefied Gas Dynamics* (Plenum, New York, 1985), Vol. 1, pp. 313–332.
22. Yu. I. Khlopkov, "Solution of the Linearized Boltzmann Equation," Zh. Vychisl. Mat. Mat. Fiz. **13**, 1307–1314 (1973).
23. Yu. I. Khlopkov and A. S. Kravchuk, "Simulation of Rarefied Gas Flow and of a Continuum," in *Proc. XVII Int. Symp. on Rarefied Gas Dynamics* (RWTH, Aachen, 1990) Vol. 1, p. 332.
24. M. N. Kogan, A. S. Kravchuk, and Yu. I. Khlopkov, "The Relaxation–Transfer Method in Gas Dynamics for a Wide Range of Rarefaction of the Medium," Uchenyi Zapiski Tsentr. Aerogidrodinamicheskogo Inst. **19** (2), 106–109 (1988).
25. S. L. Gorelov, V. A. Zharov, and Yu. I. Khlopkov, "The Kinetic Approaches to the Turbulence Description," in *Proc. XX Int. Symp. on Rarefied Gas Dynamics* (Peking, 1997), pp. 192–199.
26. M. A. Rutgers, "Forced 2D Turbulence: Experimental Evidence of Simultaneous Inverse Energy and Forward Enstrophy Cascades," Phys. Rev. Lett. **81**, 2244–2247 (1998).
27. A. Sakurai and F. Takayama, "Molecular Kinetic Approach to the Problem of Compressible Turbulence," Phys. Fluids **15**, 1282–1294 (2003).
28. Yu. I. Khlopkov, I. V. Voronich, and O. I. Rovenskaya, "Numerical Simulation of Nonlinear Effects in a Compressible Gas Based on the Navier–Stokes and Kinetic Equations," in *Abstracts II Int. Conf. Aviation Motors of the XXI Century* (Central Institute of Aviation Motors, Moscow, 2005), pp. 146–149 [in Russian].
29. B. N. Chetverushkin, *Kinetically Consistent Difference Schemes in Gas Dynamics* (Mosk. Gos. Univ., Moscow, 1999) [in Russian].